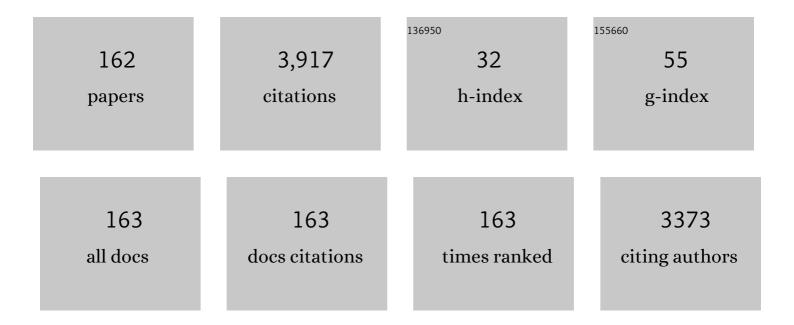
Khalid Hattar

List of Publications by Year in descending order

Source: https://exaly.com/author-pdf/2686364/publications.pdf Version: 2024-02-01



ΚΗΛΙΙΟ ΗΛΤΤΛΡ

#	Article	IF	CITATIONS
1	Radiation damage in nanostructured materials. Progress in Materials Science, 2018, 96, 217-321.	32.8	307
2	Characterisation of radiation damage in W and W-based alloys from 2 MeV self-ion near-bulk implantations. Acta Materialia, 2015, 92, 163-177.	7.9	159
3	Influence of interfaces on the storage of ion-implanted He in multilayered metallic composites. Journal of Applied Physics, 2005, 98, 123516.	2.5	149
4	Experimental Investigation of Size Effects on the Thermal Conductivity of Silicon-Germanium Alloy Thin Films. Physical Review Letters, 2012, 109, 195901.	7.8	138
5	Helium bubble formation in ultrafine and nanocrystalline tungsten under different extreme conditions. Journal of Nuclear Materials, 2015, 458, 216-223.	2.7	137
6	Towards data-driven next-generation transmission electron microscopy. Nature Materials, 2021, 20, 274-279.	27.5	130
7	Arrest of He bubble growth in Cu–Nb multilayer nanocomposites. Scripta Materialia, 2008, 58, 541-544.	5.2	111
8	Concurrent in situ ion irradiation transmission electron microscope. Nuclear Instruments & Methods in Physics Research B, 2014, 338, 56-65.	1.4	111
9	A high electromechanical coupling coefficient SH0 Lamb wave lithium niobate micromechanical resonator and a method for fabrication. Sensors and Actuators A: Physical, 2014, 209, 183-190.	4.1	96
10	Do voids nucleate at grain boundaries during ductile rupture?. Acta Materialia, 2017, 137, 103-114.	7.9	79
11	Anisotropic radiation-induced segregation in 316L austenitic stainless steel with grain boundary character. Acta Materialia, 2014, 67, 145-155.	7.9	74
12	The role of grain size in He bubble formation: Implications for swelling resistance. Journal of Nuclear Materials, 2017, 484, 236-244.	2.7	70
13	Grain boundary phase transformations in PtAu and relevance to thermal stabilization of bulk nanocrystalline metals. Journal of Materials Science, 2018, 53, 2911-2927.	3.7	65
14	Direct Observation of Sink-Dependent Defect Evolution in Nanocrystalline Iron under Irradiation. Scientific Reports, 2017, 7, 1836.	3.3	57
15	Ion irradiation of the native oxide/silicon surface increases the thermal boundary conductance across aluminum/silicon interfaces. Physical Review B, 2014, 90, .	3.2	53
16	In-situ TEM/heavy ion irradiation on ultrafine-and nanocrystalline-grained tungsten: Effect of 3 MeV Si, Cu and W ions. Materials Characterization, 2015, 99, 68-76.	4.4	53
17	Defect character at grain boundary facet junctions: Analysis of an asymmetric ΣÂ=Â5 grain boundary in Fe. Acta Materialia, 2017, 124, 383-396.	7.9	49
18	Thermal conductivity measurements via time-domain thermoreflectance for the characterization of radiation induced damage. Journal of Materials Research, 2015, 30, 1403-1412.	2.6	47

#	Article	IF	CITATIONS
19	Microstructure, chemistry and mechanical properties of Ni-based superalloy Rene N4 under irradiation at room temperature. Acta Materialia, 2015, 95, 357-365.	7.9	46
20	High Cycle Fatigue in the Transmission Electron Microscope. Nano Letters, 2016, 16, 4946-4953.	9.1	46
21	Defect structures created during abnormal grain growth in pulsed-laser deposited nickel. Acta Materialia, 2008, 56, 794-801.	7.9	45
22	Detecting self-ion irradiation-induced void swelling in pure copper using transient grating spectroscopy. Acta Materialia, 2018, 145, 496-503.	7.9	44
23	Spectral- and Pulse-Shape Discrimination in Triplet-Harvesting Plastic Scintillators. IEEE Transactions on Nuclear Science, 2012, 59, 3312-3319.	2.0	41
24	In situ study of heavy ion irradiation response of immiscible Cu/Fe multilayers. Journal of Nuclear Materials, 2016, 475, 274-279.	2.7	41
25	Thermal Stability Comparison of Nanocrystalline Fe-Based Binary Alloy Pairs. Jom, 2016, 68, 1625-1633.	1.9	41
26	In-Situ Transmission Electron Microscopy of Liposomes in an Aqueous Environment. Langmuir, 2013, 29, 9958-9961.	3.5	40
27	Study of rapid grain boundary migration in a nanocrystalline Ni thin film. Materials Science & Engineering A: Structural Materials: Properties, Microstructure and Processing, 2011, 528, 1628-1635.	5.6	39
28	Room Temperature Deformation Mechanisms of Alumina Particles Observed from In Situ Micro-compression and Atomistic Simulations. Journal of Thermal Spray Technology, 2016, 25, 82-93.	3.1	39
29	In situ Transmission Electron Microscopy Observations of Toughening Mechanisms in Ultra-fine Grained Columnar Aluminum Thin Films. Journal of Materials Research, 2005, 20, 1869-1877.	2.6	36
30	Early stage damage of ultrafine-grained tungsten materials exposed to low energy helium ion irradiation. Fusion Engineering and Design, 2015, 93, 9-14.	1.9	36
31	The role of grain boundary character in solute segregation and thermal stability of nanocrystalline Pt–Au. Nanoscale, 2021, 13, 3552-3563.	5.6	35
32	The onset and evolution of fatigue-induced abnormal grain growth in nanocrystalline Ni–Fe. Journal of Materials Science, 2017, 52, 46-59.	3.7	34
33	Grain boundary character dependence of radiation-induced segregation in a model Ni–Cr alloy. Journal of Materials Research, 2015, 30, 1290-1299.	2.6	33
34	Solute stabilization of nanocrystalline tungsten against abnormal grain growth. Journal of Materials Research, 2018, 33, 68-80.	2.6	33
35	Irradiation induced creep in nanocrystalline high entropy alloys. Acta Materialia, 2020, 182, 68-76.	7.9	32
36	In situ probing of the evolution of irradiation-induced defects in copper. Journal of Nuclear Materials, 2013, 439, 185-191.	2.7	31

#	Article	IF	CITATIONS
37	In situ measurements of a homogeneous to heterogeneous transition in the plastic response of ion-irradiated ã€^1 1 1〉 Ni microspecimens. Acta Materialia, 2015, 88, 121-135.	7.9	31
38	The role of the interface stiffness tensor on grain boundary dynamics. Acta Materialia, 2018, 158, 440-453.	7.9	31
39	The Effect of He Implantation on the Tensile Properties and Microstructure of Cu/Fe Nanoâ€Bicrystals. Advanced Functional Materials, 2013, 23, 1281-1288.	14.9	30
40	High temperature irradiation induced creep in Ag nanopillars measured via in situ transmission electron microscopy. Scripta Materialia, 2018, 148, 1-4.	5.2	28
41	Evidence of a temperature transition for denuded zone formation in nanocrystalline Fe under He irradiation. Materials Research Letters, 2017, 5, 195-200.	8.7	27
42	New nanoscale toughening mechanisms mitigate embrittlement in binary nanocrystalline alloys. Nanoscale, 2018, 10, 21231-21243.	5.6	27
43	Heavy ion irradiation effects on GaN/AlGaN high electron mobility transistor failure at off-state. Microelectronics Reliability, 2019, 102, 113493.	1.7	27
44	Real-time thermomechanical property monitoring during ion beam irradiation using in situ transient grating spectroscopy. Nuclear Instruments & Methods in Physics Research B, 2019, 440, 126-138.	1.4	27
45	Orders of magnitude reduction in the thermal conductivity of polycrystalline diamond through carbon, nitrogen, and oxygen ion implantation. Carbon, 2020, 157, 97-105.	10.3	27
46	Hierarchical nanotwins in single-crystal-like nickel with high strength and corrosion resistance produced <i>via</i> a hybrid technique. Nanoscale, 2020, 12, 1356-1365.	5.6	27
47	Unraveling irradiation induced grain growth with <i>in situ</i> transmission electron microscopy and coordinated modeling. Applied Physics Letters, 2015, 107, .	3.3	26
48	Reduction in thermal boundary conductance due to proton implantation in silicon and sapphire. Applied Physics Letters, 2011, 98, 231901.	3.3	25
49	The role of copper twin boundaries in cryogenic indentation-induced grain growth. Materials Science & Engineering A: Structural Materials: Properties, Microstructure and Processing, 2014, 592, 182-188.	5.6	24
50	Irradiation-induced creep in metallic nanolaminates characterized by In situ TEM pillar nanocompression. Journal of Nuclear Materials, 2017, 490, 59-65.	2.7	24
51	Suppressing irradiation induced grain growth and defect accumulation in nanocrystalline tungsten through grain boundary doping. Acta Materialia, 2021, 206, 116629.	7.9	24
52	Examining the influence of grain size on radiation tolerance in the nanocrystalline regime. Applied Physics Letters, 2018, 112, .	3.3	23
53	In Situ Transmission Electron Microscopy for Ultrahigh Temperature Mechanical Testing of ZrO ₂ . Nano Letters, 2020, 20, 1041-1046.	9.1	23
54	Competitive Abnormal Grain Growth between Allotropic Phases in Nanocrystalline Nickel. Advanced Materials, 2010, 22, 1161-1164.	21.0	22

#	Article	IF	CITATIONS
55	Compressive Properties of ⟠110⟩ Cu Micro-Pillars after High-Dose Self-Ion Irradiation. Materials Research Letters, 2014, 2, 57-62.	8.7	22
56	Interplay Between Grain Boundaries and Radiation Damage. Jom, 2019, 71, 1233-1244.	1.9	22
57	Phonon scattering effects from point and extended defects on thermal conductivity studied via ion irradiation of crystals with self-impurities. Physical Review Materials, 2018, 2, .	2.4	22
58	Ion beam modification of topological insulator bismuth selenide. Applied Physics Letters, 2014, 105, .	3.3	21
59	Synthesis and Characterization of Solvothermal Processed Calcium Tungstate Nanomaterials from Alkoxide Precursors. Chemistry of Materials, 2014, 26, 965-975.	6.7	21
60	Thermal flux limited electron Kapitza conductance in copper-niobium multilayers. Applied Physics Letters, 2015, 106, .	3.3	21
61	Fatigue and fracture of nanostructured metals and alloys. MRS Bulletin, 2021, 46, 258-264.	3.5	21
62	Thermal stability of Ni/NiO multilayers. Materials Science & Engineering A: Structural Materials: Properties, Microstructure and Processing, 2013, 568, 49-60.	5.6	20
63	Amorphous intergranular films mitigate radiation damage in nanocrystalline Cu-Zr. Acta Materialia, 2020, 186, 341-354.	7.9	20
64	Direct Observation of Crack Propagation in Copper–Niobium Multilayers. Journal of Engineering Materials and Technology, Transactions of the ASME, 2012, 134, .	1.4	19
65	Characterizing single isolated radiation-damage events from molecular dynamics via virtual diffraction methods. Journal of Applied Physics, 2018, 123, .	2.5	19
66	Irradiation-induced grain boundary facet motion: In situ observations and atomic-scale mechanisms. Science Advances, 2022, 8, .	10.3	18
67	A diffuse interface model of grain boundary faceting. Journal of Applied Physics, 2016, 119, 235306.	2.5	17
68	Evidence that abnormal grain growth precedes fatigue crack initiation in nanocrystalline Ni-Fe. Scripta Materialia, 2018, 143, 15-19.	5.2	17
69	Observations of defect structure evolution in proton and Ni ion irradiated Ni-Cr binary alloys. Journal of Nuclear Materials, 2016, 479, 48-58.	2.7	16
70	Cavity Evolution at Grain Boundaries as a Function of Radiation Damage and Thermal Conditions in Nanocrystalline Nickel. Materials Research Letters, 2016, 4, 96-103.	8.7	16
71	In situ TEM investigation of self-ion irradiation of nanoporous gold. Journal of Materials Science, 2019, 54, 7271-7287.	3.7	16
72	Electrostatic subframing and compressive-sensing video in transmission electron microscopy. Structural Dynamics, 2019, 6, 054303.	2.3	16

#	Article	IF	CITATIONS
73	In Situ Study of Particle Precipitation in Metal-Doped CeO ₂ during Thermal Treatment and Ion Irradiation for Emulation of Irradiating Fuels. Journal of Physical Chemistry C, 2019, 123, 2591-2601.	3.1	16
74	Ultrahigh temperature in situ transmission electron microscopy based bicrystal coble creep in Zirconia II: Interfacial thermodynamics and transport mechanisms. Acta Materialia, 2020, 200, 1008-1021.	7.9	16
75	Development of a heterogeneous nanostructure through abnormal recrystallization of a nanotwinned Ni superalloy. Acta Materialia, 2020, 195, 132-140.	7.9	16
76	Initial texture effects on the thermal stability and grain growth behavior of nanocrystalline Ni thin films. Materials Science & Engineering A: Structural Materials: Properties, Microstructure and Processing, 2016, 675, 110-119.	5.6	15
77	Metastable Tantalum Oxide Formation During the Devitrification of Amorphous Tantalum Thin Films. Journal of the American Ceramic Society, 2016, 99, 3775-3783.	3.8	15
78	Defect evolution in Ni and NiCoCr by in situ 2.8â€ [−] MeV Au irradiation. Journal of Nuclear Materials, 2019, 523, 502-509.	2.7	15
79	Ultrahigh temperature in situ transmission electron microscopy based bicrystal coble creep in zirconia I: Nanowire growth and interfacial diffusivity. Acta Materialia, 2020, 199, 530-541.	7.9	15
80	Possibility of an integrated transmission electron microscope: enabling complex in-situ experiments. Journal of Materials Science, 2021, 56, 5309-5320.	3.7	15
81	Exploring Coupled Extreme Environments via <i>In-situ</i> Transmission Electron Microscopy. Microscopy Today, 2021, 29, 28-34.	0.3	14
82	In situ TEM ion irradiation and implantation effects on Au nanoparticle morphologies. Chemical Communications, 2014, 50, 7593.	4.1	13
83	<i>In Situ</i> TEM Concurrent and Successive Au Self-Ion Irradiation and He Implantation. Materials Transactions, 2014, 55, 418-422.	1.2	12
84	Layer-Dependent Bit Error Variation in 3-D NAND Flash Under Ionizing Radiation. IEEE Transactions on Nuclear Science, 2020, 67, 2021-2027.	2.0	12
85	Stability of immiscible nanocrystalline alloys in compositional and thermal fields. Acta Materialia, 2022, 226, 117620.	7.9	12
86	In Situ TEM Multi-Beam Ion Irradiation as a Technique for Elucidating Synergistic Radiation Effects. Materials, 2017, 10, 1148.	2.9	11
87	Effect of friction stir welding and self-ion irradiation on dispersoid evolution in oxide dispersion strengthened steel MA956 up to 25 dpa. Journal of Nuclear Materials, 2019, 515, 407-419.	2.7	11
88	Displacement rate and temperature equivalence in stochastic cluster dynamics simulations of irradiated pure α-Fe. Journal of Nuclear Materials, 2016, 480, 129-137.	2.7	10
89	Direct observation of a coincident dislocation- and grain boundary-mediated deformation in nanocrystalline iron. Materials Science & Engineering A: Structural Materials: Properties, Microstructure and Processing, 2018, 709, 339-348.	5.6	10
90	Application of In Situ TEM to Investigate Irradiation Creep in Nanocrystalline Zirconium. Jom, 2019, 71, 3350-3357.	1.9	10

#	Article	IF	CITATIONS
91	In Situ High-Cycle Fatigue Reveals Importance of Grain Boundary Structure in Nanocrystalline Cu-Zr. Jom, 2019, 71, 1221-1232.	1.9	10
92	Radiation-Induced Error Mitigation by Read-Retry Technique for MLC 3-D NAND Flash Memory. IEEE Transactions on Nuclear Science, 2021, 68, 1032-1039.	2.0	10
93	Physical response of gold nanoparticles to single self-ion bombardment. Journal of Materials Research, 2014, 29, 2387-2397.	2.6	9
94	Effects of crystallographic and geometric orientation on ion beam sputtering of gold nanorods. Scientific Reports, 2018, 8, 512.	3.3	9
95	Investigations of irradiation effects in crystalline and amorphous SiC. Journal of Applied Physics, 2019, 126, .	2.5	9
96	Rethinking scaling laws in the high-cycle fatigue response of nanostructured and coarse-grained metals. International Journal of Fatigue, 2020, 134, 105472.	5.7	9
97	Size-dependent radiation damage mechanisms in nanowires and nanoporous structures. Acta Materialia, 2021, 215, 117018.	7.9	9
98	In situ Transmission Electron Microscopy He+ implantation and thermal aging of nanocrystalline iron. Journal of Nuclear Materials, 2016, 482, 139-146.	2.7	8
99	Impact of oleylamine: oleic acid ratio on the morphology of yttria nanomaterials. Journal of Materials Science, 2017, 52, 8268-8279.	3.7	8
100	Investigating Helium Bubble Nucleation and Growth through Simultaneous In-Situ Cryogenic, Ion Implantation, and Environmental Transmission Electron Microscopy. Materials, 2019, 12, 2618.	2.9	8
101	Listening to Radiation Damage In Situ: Passive and Active Acoustic Techniques. Jom, 2020, 72, 197-209.	1.9	8
102	Using In Situ TEM Helium Implantation and Annealing to Study Cavity Nucleation and Growth. Jom, 2020, 72, 2032-2041.	1.9	8
103	Gamma-Ray-Induced Error Pattern Analysis for MLC 3-D NAND Flash Memories. IEEE Transactions on Nuclear Science, 2021, 68, 733-739.	2.0	8
104	In situ ion irradiation of amorphous TiO2 nanotubes. Journal of Materials Research, 2022, 37, 1144-1155.	2.6	8
105	Unexpected radiation resistance of core/shell ceramic oxide nanoparticles. Materials Today Communications, 2018, 17, 109-113.	1.9	7
106	Analytical Bit-Error Model of NAND Flash Memories for Dosimetry Application. IEEE Transactions on Nuclear Science, 2022, 69, 478-484.	2.0	7
107	Electron Beam Effects during In-Situ Annealing of Self-Ion Irradiated Nanocrystalline Nickel. Materials Research Society Symposia Proceedings, 2015, 1809, 13-18.	0.1	6
108	The influence of solute on irradiation damage evolution in nanocrystalline thin-films. Journal of Nuclear Materials, 2021, 543, 152616.	2.7	6

#	Article	IF	CITATIONS
109	Probing thermal conductivity of subsurface, amorphous layers in irradiated diamond. Journal of Applied Physics, 2021, 129, .	2.5	6
110	Percolation of Ion-Irradiation-Induced Disorder in Complex Oxide Interfaces. Nano Letters, 2021, 21, 5353-5359.	9.1	6
111	Total Ionizing Dose Effects on Long-Term Data Retention Characteristics of Commercial 3-D NAND Memories. IEEE Transactions on Nuclear Science, 2022, 69, 390-396.	2.0	6
112	Implications of Microstructure in Helium-Implanted Nanocrystalline Metals. Materials, 2022, 15, 4092.	2.9	6
113	He implantation for improved tribological performance in Au electrical contacts. Journal of Materials Science, 2015, 50, 382-392.	3.7	5
114	Novel amorphous SiOC dispersion-strengthened austenitic steels. Materialia, 2019, 6, 100345.	2.7	5
115	Additive manufacturing assisted van der Waals integration of 3D/3D hierarchically functional nanostructures. Communications Materials, 2020, 1, .	6.9	5
116	In Situ TEM Study of Radiation Resistance of Metallic Glass–Metal Core–Shell Nanocubes. ACS Applied Materials & Interfaces, 2020, 12, 40910-40916.	8.0	5
117	Statistical analysis of the interaction between irradiation-induced defects and triple junctions. Advanced Modeling and Simulation in Engineering Sciences, 2020, 7, .	1.7	5
118	A combined thermomechanical and radiation testing platform for a 6 MV tandem accelerator. Nuclear Instruments & Methods in Physics Research B, 2021, 509, 39-47.	1.4	5
119	Compositional Effects of Additively Manufactured Refractory High-Entropy Alloys under High-Energy Helium Irradiation. Nanomaterials, 2022, 12, 2014.	4.1	5
120	Self-ion irradiation effects on mechanical properties of nanocrystalline zirconium films. MRS Communications, 2017, 7, 595-600.	1.8	4
121	Synthesis of complex rare earth nanostructures using in situ liquid cell transmission electron microscopy. Nanoscale Advances, 2019, 1, 2229-2239.	4.6	4
122	Helium Bubbles and Blistering in a Nanolayered Metal/Hydride Composite. Materials, 2021, 14, 5393.	2.9	4
123	The dynamic evolution of swelling in nickel concentrated solid solution alloys through inÂsitu property monitoring. Applied Materials Today, 2021, 25, 101187.	4.3	4
124	The In Situ Ion Irradiation Toolbox: Time-Resolved Structure and Property Measurements. Jom, 2022, 74, 126.	1.9	4
125	Thermal Stability and Radiation Tolerance of Lanthanide-Doped Cerium Oxide Nanocubes. Crystals, 2021, 11, 1369.	2.2	4
126	Solute segregation improves the high-cycle fatigue resistance of nanocrystalline Pt-Au. Acta Materialia, 2022, 229, 117794.	7.9	4

#	Article	IF	CITATIONS
127	Ion beam characterization of advanced luminescent materials for application in radiation effects microscopy. Nuclear Instruments & Methods in Physics Research B, 2011, 269, 2326-2329.	1.4	3
128	Using <i>in-situ</i> TEM Triple Ion Beam Irradiations to Study the Effects of Deuterium, Helium, and Radiation Damage on TPBAR Component s . Microscopy and Microanalysis, 2017, 23, 2216-2217.	0.4	3
129	Total Ionizing Dose Effects on Physical Unclonable Function From NAND Flash Memory. IEEE Transactions on Nuclear Science, 2021, 68, 1445-1453.	2.0	3
130	Evidence for a High Temperature Whisker Growth Mechanism Active in Tungsten during In Situ Nanopillar Compression. Nanomaterials, 2021, 11, 2429.	4.1	3
131	Pulsed electric current joining of oxide-dispersion-strengthened austenitic steels. Journal of Materials Science, 2021, 56, 19216-19227.	3.7	3
132	Photo-exfoliation of MoS ₂ quantum dots from nanosheets: an in situ transmission electron microscopy study. Nanotechnology, 2022, 33, 085601.	2.6	3
133	Length Scale Effect on Deformation and Failure Mechanisms of Ultra-Fine Grained Aluminum. Materials Research Society Symposia Proceedings, 2005, 907, 1.	0.1	2
134	Thermal conductivity of self-ion irradiated nanocrystalline zirconium thin films. Thin Solid Films, 2017, 638, 17-21.	1.8	2
135	A study of irradiation effects in TiO2 using molecular dynamics simulation and complementary in situ transmission electron microscopy. Journal of Applied Physics, 2018, 124, 095901.	2.5	2
136	Evolution of Gold Nanoparticles in Radiation Environments. , 0, , .		2
137	Watching High-Cycle Fatigue with Automated Scanning Electron Microscope Experiments. Conference Proceedings of the Society for Experimental Mechanics, 2021, , 73-76.	0.5	2
138	Reductions in the thermal conductivity of irradiated silicon governed by displacement damage. Physical Review B, 2021, 104, .	3.2	2
139	Applications of Liquid Cell-TEM in Corrosion Research. , 2022, , 121-150.		2
140	Total Ionizing Dose Effects on Read Noise of MLC 3-D NAND Memories. IEEE Transactions on Nuclear Science, 2022, 69, 321-326.	2.0	2
141	Fabrication, thermal analysis, and heavy ion irradiation resistance of epoxy matrix nanocomposites loaded with silane-functionalized ceria nanoparticles. Physical Chemistry Chemical Physics, 2022, 24, 6552-6569.	2.8	2
142	Unraveling Thermodynamic and Kinetic Contributions to the Stability of Doped Nanocrystalline Alloys using Nanometallic Multilayers. Advanced Materials, 2022, 34, e2200354.	21.0	2
143	Mechanisms of Grain Growth in Free-Standing Nanograined Gold Thin Films. Materials Research Society Symposia Proceedings, 2005, 907, 1.	0.1	1
144	Cavity Formation in Molybdenum Studied In Situ in TEM. Fusion Science and Technology, 2017, 71, 268-274.	1.1	1

#	Article	IF	CITATIONS
145	In-situ Ion Irradiation and Recrystallization in Highly Structured Materials. Microscopy and Microanalysis, 2019, 25, 1572-1573.	0.4	1
146	Demonstration of elastic recoil detection as a technique for quantifying 6Li burnup in tritium breeder materials. AIP Conference Proceedings, 2019, , .	0.4	1
147	In-situ TEM irradiation induced amorphization of Ge2Sb2Te5. Microscopy and Microanalysis, 2021, 27, 1232-1234.	0.4	1
148	Automated Crystal Orientation Mapping with a Liquid-Cell TEM. Microscopy and Microanalysis, 2021, 27, 2232-2233.	0.4	1
149	Microstructural effects of high dose helium implantation in ErD2. Materialia, 2022, 22, 101280.	2.7	1
150	Friction stir welding and self-ion irradiation effects on microstructure and mechanical properties changes within oxide dispersion strengthened steel MA956. Journal of Nuclear Materials, 2022, 567, 153795.	2.7	1
151	New Total-Ionizing-Dose Resistant Data Storing Technique for NAND Flash Memory. IEEE Transactions on Device and Materials Reliability, 2022, 22, 438-446.	2.0	1
152	In situ TEM Observations of Grain Growth in Nanograined Thin Films. Materials Research Society Symposia Proceedings, 2004, 854, U6.6.1.	0.1	0
153	In Situ Observation of Single Ion Damage in Electronic Materials. Microscopy and Microanalysis, 2015, 21, 1013-1014.	0.4	Ο
154	Minimal Variation of Defect Structure Due to the Order of Room Temperature Hydrogen Isotope Implantation and Self-Ion Irradiation in Nickel. MRS Advances, 2016, 1, 2887-2892.	0.9	0
155	Application of In-situ TEM Nanoscale Quantitative Mechanical Testing to Elastomers. Microscopy and Microanalysis, 2019, 25, 1524-1525.	0.4	Ο
156	Initiation of Grain Growth Observed Using Electrostatic-Subframing. Microscopy and Microanalysis, 2019, 25, 1518-1519.	0.4	0
157	Development of the In-Situ Ion Irradiation SEM at Sandia National Laboratories. Microscopy and Microanalysis, 2019, 25, 1596-1597.	0.4	0
158	In-situ Irradiation, Helium Implantation and Heating to Elucidate Mechanisms in Tungsten Alloys. Microscopy and Microanalysis, 2021, 27, 2636-2638.	0.4	0
159	Thickness and Surface Effects on Abnormal Grain Growth in Nanocrystalline Nickel Films. , 2016, , 253-258.		0
160	Exploring Coupled Extreme Environments via In-situ Transmission Electron Microscopy. Microscopy and Microanalysis, 2020, 26, 876-877.	0.4	0
161	In-situ High Temperature Ion Irradiation Transmission Electron Microscopy to Understand Fission Product Transport in Silicon Carbide of TRISO Fuel. Microscopy and Microanalysis, 2020, 26, 870-871.	0.4	0
162	Crystallization kinetics and thermodynamics of an Ag–In–Sb–Te phase change material using complementary in situ microscopic techniques. Journal of Materials Research, 2022, 37, 1281.	2.6	0